JOURNAL OF AGRICULTURAL AND FOOD CHEMISTRY

Model Studies on the Release of Aroma Compounds from Structured and Nonstructured Oil Systems Using Proton-Transfer Reaction Mass Spectrometry

PASCALE LANDY,† PHILIPPE POLLIEN,† ANDREAS RYTZ,† MARTIN E. LESER,† LAURENT SAGALOWICZ,† IMRE BLANK,‡ AND JEAN-CLAUDE SPADONE*,†

Nestlé Research Center, Vers-chez-les-Blanc, CH-1000 Lausanne 26, Switzerland, and Nestlé Product Technology Center Orbe, CH-1350 Orbe, Switzerland

Relative retention, volatility, and temporal release of volatile compounds taken from aldehyde, ester, and alcohol chemical classes were studied at 70 °C in model systems using equilibrium static headspace analysis and real time dynamic headspace analysis. These systems were medium-chain triglycerides (MCT), sunflower oil, and two structured systems, i.e., water-in-oil emulsion and L_2 phase (water-in-oil microemulsion). Hydrophilic domains of the emulsion type media retained specifically the hydrophilic compounds and alcohols. Four kinetic parameters characterizing the concentration- and time-dependent releases were extracted from the aroma release curves. Most of the kinetic parameter values were higher in structured systems than in oils particularly when using MCT. The oil nature was found to better control the dynamic release profiles than the system structures. The release parameters were well-related (i) to the volatile hydrophobicity as a function of the oil used and (ii) to the retention data in the specific case of the L_2 phase due to a specific release behavior of alcohols.

KEYWORDS: Proton-transfer reaction mass spectrometry; L_2 phase; water-in-oil emulsion; partition coefficient; aroma retention; dynamic aroma release

INTRODUCTION

The aroma perception of food before and during consumption is a critical factor driving consumer preference and repeat-buying behavior. It is now recognized that in order to obtain good sensory perception, aroma compounds have to be delivered at the appropriate rate and profiles over time (*1*, *2*). A burst of flavor and its lingering effect upon food preparation and consumption are temporal, and desired phenomena are provided by the differential release of volatiles (*3*, *4*). Dynamic aroma release patterns change significantly as a function of the physicochemical characteristics of the volatiles (*5*), the food matrix composition (*6*), the matrix structure, and the aroma−matrix interactions (*7*).

Lipid phases are ingredients of many food products and are widely known to affect aroma release and perception as well as the food structure and mouthfeel (*8*). Basically, the hydrophobic nature of aroma compounds leads to their partitioning into lipids and therefore to a reduction of their concentration and odor intensity into the gas phase, while the headspace intensity of hydrophilic compounds increases (*9*). Aroma release from bulk oils (*10*), oil-in-water (o/w) (*11*), and water-in-oil (w/o) emulsions (*12*, *13*) has been largely investigated in order to understand the influence of most food structures on the mechanisms governing flavor release and delivery. Under dynamic conditions, lipids appear to act as a flavor reservoir and induce a time-dependent aroma release resulting in a delayed perception (*5*, *14*). These studies showed how lipids and emulsions modulate flavor release and perception.

Single or multiple (e.g., w/o/w) emulsions, therefore, constitute aroma delivery systems of great interest combining hydrophilic and hydrophobic domains and exhibiting a potential of controlled release properties (*15*, *16*). The introduction of a diffusional lipid barrier and interfacial resistances to mass transfer between the aqueous phase and the gas (or liquid) phase is expected to reduce the transfer rate of hydrophilic compounds, thus controlling their release (*13*, *17*).

Water-in-oil microemulsions (or L_2 phases) are also ternary systems (water, oil, and surfactant) presenting hydrophobic and hydrophobic properties, but they differ fundamentally from emulsions with respect to their formation and stability (*18*). The microemulsion constituents organize themselves autonomously into patterns, which are governed by the interactions exerted between the components in the system. Microemulsions are, therefore, thermodynamically stable and form a self-assembly structure (*19*). In contrast, w/o emulsions are thermodynamically unstable and separate into a distinct lipid and water phase as a function of time. The other characteristic difference between

* To whom correspondence should be addressed. E-mail: jean-claude.spadone@rdls.nestle.com.
† Nestlé Research Center.
‡ Nestlé Product Technology Center Orbe.

10.1021/jf062643p CCC: $37.00
Published on Web 01/31/2007

emulsions and microemulsions is their appearance. An emulsion is turbid while a microemulsion is transparent. This visual difference in appearance is directly linked to the water droplet size, being in the range of 100−1000 nm for w/o emulsions and 1−100 nm for w/o microemulsions (*18*). Some patents have been issued on the application of microemulsions and other self-assembly structures in the food industry (*3*, *20*, *21*). However, no work has been reported on the release of aroma compounds from microemulsions.

In the present study, the effect of structured lipid-containing systems on the dynamic aroma release was evaluated by means of on-line real-time measurements using a direct mass spectrometry method, i.e., proton-transfer reaction mass spectrometry (PTR-MS). Water-in-oil emulsions and w/o microemulsions were compared relatively to a reference system, i.e., a bulk oil phase. A second objective of the work was to investigate how a change in the lipid type could influence the aroma release from these systems. Medium-chain triglycerides (MCT) and sunflower oil were chosen for their difference in chain length and degree of saturation. An aroma−matrix interaction study was conducted in order to determine the influence of these interactions on the aroma release profiles. A model system of aroma compounds was selected in order to provide a better insight into the physicochemical properties of the volatiles that control the release from bulk oil systems, w/o emulsions, and microemulsions. All instrumental measurements were conducted at 70 °C to simulate aroma release and perception during the preparation or reconstitution of hot food products.

MATERIALS AND METHODS

Aroma Compounds. Acetaldehyde, methyl formate, ethyl butanoate, 1-octanol, nonanal, and decanal were purchased from Fluka (Buchs, Switzerland); 1-butanol and hexanal were from Aldrich-Sigma (Steinheim, Germany); and ethyl acetate was from Merck (Darmstadt, Germany). The concentrations of the nine aroma compounds were chosen so that the fragment ions of the different aroma compounds could give a detectable instrumental signal and had no interference between each other. The concentrations of the aroma compounds in μL/L were as follows: 5 for acetaldehyde, 5 for methyl formate, 50 for butanol, 50 for ethyl acetate, 40 for hexanal, 5 for ethyl butanoate, 400 for octanol, 800 for nonanal, and 1000 for decanal.

Preparations of Samples. *Oils*. MCT oil (Delios V, Cognis, Illertissen, Germany) and sunflower oil (Oleificio Sabo, Manno, Switzerland) were used to prepare the three investigated matrices: 100% oil system, L_2 phase, and w/o emulsion.

Pure Oil Systems. The pure oil systems were prepared by dissolving the aroma compounds in oil.

L_2 Phases. The microemulsions were constituted of 10% water, 30% unsaturated monoglycerides (Dimodan U/J, Danisco, Grinsted, Denmark), 60% oil, and the nine aroma compounds. The mixture was heated to 70 °C for 5 min and manually shaken. The samples were then cooled down to room temperature in order to form the microemulsion.

Emulsions. The w/o emulsions were composed of 10% water, 5% polyglycerol polyricinoleate (PGPR 90, Danisco), 85% oil, and the nine aroma compounds. Emulsification was performed by homogenization (Ultra-Turrax, 2 min, 20500 rpm).

Liquid−Air Partition Coefficient Determination. The liquid−air partition coefficients of the aroma compounds in oil at 70 °C were determined using a dynamic technique as reported by Leroi et al. (*22*) and Mackay et al. (*23*). This stripping method was adapted to perform the on-line measurement of the volatile compound concentration in the headspace by PTR-MS (*24*, *25*).

For all considered volatile compounds, except decanal, a single stripping cell configuration was used. The compound concentrations in MCT or sunflower oil varied from 2 (acetaldehyde and methyl formate) to 600 μL/L (nonanal) depending on the compound solubility and volatility in oil. Air was introduced into a stripping cell containing 100 mL of oil (40 cm liquid height) at flow rates ranging from 30 to 100 standard cubic centimeters per minute (sccm). Air bubbles were generated by means of a sintered glass disk (two disks were tested) or a nozzle (10 cylindrical holes of 0.18 mm diameter) designed as described by Pollien et al. (*25*). The pore diameter of the sintered glass disks ranged from 17 to 40 and from 101 to 160 μm. The liquid−air equilibrium reached in the bubbles depended on the bubble size and their residence time within the liquid. The residence time was given by both the liquid height (optimized and fixed at 40 cm) and the vertical speed of the bubbles governed by their size (*24*). The stripping gas flow rate was adjusted to minimize the air bubble diameter inside the oil phase, i.e., in the range of 2−3 mm. A PTR-MS (Ionicon, Innsbruck, Austria) was used to measure the decrease of the volatile compound concentrations in the stripping gas.

A double stripping cell setup was used to determine the volatility of decanal in oil. The first stripping cell was filled with the flavored oil (4000 μL/L decanal), while the second cell (connected to the first one) contained pure oil. The air stream (100 sccm flow rate) stripped the volatile aroma compound from the first cell and enriched the oil of the second cell with the compound on the way through the cell (*24*). The increasing volatile compound concentration in the stripping gas leaving the second cell was measured on-line to determine the compound volatility. The double cell configuration was more adapted to the measurement of compounds of medium to low volatility because of its higher accuracy and speed (24 h measurement for single cell as compared to a few hours for a double cell).

Liquid−air partition coefficients were calculated as described by Karl et al. (*24*) for the single and double cell methodology. Volatility determinations were performed in 2−4 replicates. Variation coefficients ranged from 4 to 13%.

Dynamic Aroma Release Measurement. The experimental setup used for the dynamic aroma release measurements has been fully described previously (*26*, *27*). Samples of 100 mL were first heated to 70 °C for 10 min and poured into a water-purged double-jacketed glass cell (250 mL total volume) thermostated at 70 °C. The cell was then tightly connected to its lid with a clamp. Air was introduced into the gas inlet of the cell in order to continuously purge the headspace sample at 200 sccm. The sample was stirred at 180 rpm, and the temperature was monitored during the on-line analysis. The sample gas coming from the cell outlet was diluted by air at 5000 sccm. Purge and dilution gas flows were controlled with two flow controllers (Brooks Instruments B.V., Holland). The glass vessel was fixed inside a temperature-controlled oven (90 °C) in order to warm up the purging and dilution air and to avoid water and aroma condensation into the cell and tubings. An exhaust line released most of the gas volatiles since a small amount of sample gas was required for analysis by the detector. Only an 80 sccm fraction of sample gas was introduced into the PTR-MS drift tube.

Because the fragmentation of the volatile compound detected by PTR-MS decreases as the gas humidity increases (*28*), the sample humidity had to be maintained at the same level for each medium type. The ion m/z 37 was hence monitored because it corresponded to a water cluster coming from both the generation of primary H_3O^+ ions and the sample humidity. The L_2 phase and w/o emulsion induced the water cluster intensity, which was 10-fold higher than for pure oil systems. For pure oil systems, the dilution gas was first introduced through a stripping vessel containing water kept at 12 °C. This setup allowed the same water cluster level to be reached for all systems studied. On-line measurements were performed for 10 min in 3−5 replicates for each sample.

Tenax Trap Analysis. The sample gas released through the exhaust line was collected on a Tenax trap for the analysis of the volatile compounds. The trapping flow through the Tenax adsorbent was adjusted to 50 sccm by a membrane pump combined with a flow controller. The volatile entrapment on the Tenax trap was performed for 2 min. The entrapment time was optimized in order to adsorb sufficient amounts of all volatiles measured. The volatile compounds desorbed from the trap were then separated by gas chromatography and analyzed by PTR-MS and electron ionization−mass spectrometry (EI-MS). The simultaneous detection by the two detectors allowed a full identification of all molecules trapped during the release process

and the interpretation of the on-line spectrum obtained by PTR-MS (*27*). The Tenax trap analysis was performed on the six oil systems.

PTR-MS. The PTR-MS (Ionicon Analityk) analyzed, online, in real time the headspace gas introduced into the drift tube (*29*, *30*).

Liquid−Air Partition Coefficient. For volatility measurements, the full mass spectrum from *m*/*z* 20 to 160 was monitored by PTR-MS with a 0.2 s dwell time per mass.

On-line Release Measurement. During preliminary experiments, each volatile compound was dissolved individually in MCT oil and scanned from *m*/*z* 20 to 160, with a 0.2 s dwell time per mass, in order to determine the fragment ions of the aroma compounds studied. Nine specific masses were selected based on the scan data, i.e., *m*/*z* 45 for acetaldehyde, *m*/*z* 33 for methyl formate, *m*/*z* 57 for butanol, *m*/*z* 89 for ethyl acetate, *m*/*z* 101 for hexanal, *m*/*z* 117 for ethyl butanoate, *m*/*z* 71 for octanol, *m*/*z* 143 for nonanal, and *m*/*z* 157 for decanal.

A multiple ion detection mode was applied to monitor the on-line aroma release profiles. The volatile concentrations in the gas phase were calculated in μL/L (*30*).

Headspace Analysis by Solid-Phase Microextraction (HS-SPME). The different systems (2 g) containing the nine aroma compounds were placed in 10 mL vials. The fiber type, the equilibrium time before analysis (15, 30, and 60 min at 70 °C), and the linearity range of detection were tested to optimize the study of the aroma−matrix interaction by HS-SPME.

The polydimethylsiloxane/divinylbenzene (PDMS/DVB, 65 μm) and polydimethylsiloxane/carboxen (PDMS/CAR, 75 μm) fibers (Supelco, Bellefonte, PA) were tested using a sample of MCT oil containing the aroma compounds at the concentrations indicated in the section Aroma Compounds and incubated for 15 min at 70 °C.

The optimal linear range of the selected SPME fiber was determined by varying the concentrations of aroma compounds by a factor of 0.1, 0.5, 1, 1.5, and 2 as compared to the values given in the section Aroma Compounds.

A multipurpose sampler (MPS2, Gerstel Applications, Brielle, The Netherlands) was used to automate the SPME injections. The fiber was exposed for 1 min to the vial headspace kept at 70 °C. This short duration of fiber exposure was chosen to allow extraction mainly from the headspace and not from the sample. The fiber was then inserted into the GC injector for the volatile thermal desorption at 250 °C for 10 min (injector split after 3 min).

Gas Chromatography−Mass Spectrometry (GC-MS). *Tenax Trap Analysis.* The volatile compounds adsorbed on the Tenax trap were thermally desorbed by an automatic thermal desorber (ATD 400, Perkin-Elmer, Boston, MA) for 10 min at 250 °C. After they were cryofocused, the volatile compounds were injected into a GC-MS (Trace 2000 series GC equipped with an Automass Multi MS, Thermo Quest Ltd., Herts, United Kingdom). The volatiles were separated on a 60 m DB-Wax capillary column, 0.53 mm i.d., 1 μm film thickness (J&W Scientific, Folsom, CA). The oven temperature was kept at 20 °C for 1 min, then ramped from 20 to 220 °C at a rate of 4 °C/min, and held at 220 °C for 10 min. A split was introduced at the end of the capillary column for the coupling to the two MS detectors, EI-MS, and PTR-MS. The full technical features of the simultaneous coupling to EI-MS and PTR-MS have recently been described by Lindinger et al. (*27*).

SPME Analysis. The GC (HP 6890 series, Agilent, Avondale, PA) was coupled to a mass selective detector (MSD 5973, Agilent). The GC run started at 20 °C for 3 min, and then, the oven temperature increased at 6 °C/min to 240 °C (10 min). The mass spectrometer operated in the full scan mode (*m*/*z* 28−350) at 4.42 scans/s. The specific ion traces monitored for quantification were as follows: *m*/*z* 44 for acetaldehyde, *m*/*z* 60 for methyl formate, *m*/*z* 56 for butanol, *m*/*z* 43 for ethyl acetate, *m*/*z* 72 for hexanal, *m*/*z* 88 for ethyl butanoate, *m*/*z* 84 for octanol, *m*/*z* 98 for nonanal, and *m*/*z* 112 for decanal.

Data Analysis. The statistical data analysis was performed in two steps: extraction of the relevant parameters from the release curves and comparison of the extracted parameters between the different systems. Microsoft Excel and NCSS (*31*) were used to perform these analyses.

For each sample, the aroma release data consisted of nine ion traces recorded over 10 min. These kinetic curves were visualized using simple bivariate charts, allowing a direct description of the release behavior.

Table 1. Hydrophobicity and Air–Oil Partition Coefficients (Values × 10^5 ± Standard Deviation) of the Aroma Compounds in MCT and Sunflower Oil at 70 °C, Measured by PTR-MS with Single or Double Stripping Cells (Double Cell Setup Only for Decanal)

compound	log *P*[a]	MCT oil	sunflower oil
acetaldehyde	−0.16	2890 ± 99	3009 ± 222
methyl formate	−0.23	1883 ± 61	ND[b]
butanol	0.88	161 ± 29	ND
ethyl acetate	0.71	546 ± 1	ND
hexanal	1.97	84 ± 3	108 ± 8
ethyl butanoate	1.77	113 ± 1	ND
octanol	3.00	7.5 ± 1.0	ND
nonanal	3.56	6.1 ± 0.8	9.3 ± 0.7
decanal	4.09	1.3 ± 0.1	2.2 ± 0.4

[a] log *P* values calculated by the ACD/Log *P* DB software. [b] ND, not determined.

To further compare the samples, the following parameters were extracted from each kinetic curve: the release rate over the initial 15 s obtained by linear regression; the maximum intensity reached over 10 min (I_{max}); the time needed to reach I_{max} (t_{max}) expressing the delay for maximum intensity; and the area under the curve between 0 and 10 min (area 0−10) representing the global release intensity. Each release curve was characterized by means of 36 sample characteristics (nine masses × four parameters). The samples were compared using one-way analysis of variance applied on each sample characteristic, followed by a multiple comparison test, the Fisher's least significant difference (LSD), on a 5% significance level.

The comparison of two lipid systems A and B was visualized using one bivariate chart for each of the four extracted parameters. The specific mass of the volatiles, their hydrophobicity (expressed by the calculated logarithm of the water−octanol partition coefficient, log *P*), or their relative retention in the corresponding model systems were plotted on the *X*-axis.

As a complement, the correlation between the *X* and the *Y* values was also calculated. High correlations (positive or negative) indicated that the two compared samples showed a debalancing of the quality of the released aroma that could directly be related to the *X* values.

RESULTS AND DISCUSSION

Physicochemical Characteristics of the Aroma Compounds. The nine aroma compounds were selected from aldehyde, ester, and alcohol chemical groups with a view of providing different physicochemical characteristics, such as molecular weight and octanol−water partition coefficient (log *P*) (**Table 1**). The latter is considered as a theoretical constant expressing the volatile hydrophobicity. The higher the log *P* value is, the more hydrophobic is the aroma compound. Values of log *P* and molecular weight of the volatiles selected were linearly well-correlated ($r = 0.97$). In this paper, the release behavior of the aroma compounds selected was then discussed relative to their hydrophobicity.

Air−Oil Partition Coefficient (K). The partition coefficient of the aroma compounds between air and oil was measured to characterize their affinity for the two oils at 70 °C (**Table 1**). As expected, the air−oil partition coefficient of the nine compounds decreased with increasing hydrophobicity. The molecule hydrophobicity was well-related to the natural logarithm of their volatility (ln *K*), i.e., $r > 0.98$ in MCT and sunflower oils.

The homologous series of aldehydes demonstrated a higher partition coefficient in sunflower oil than in MCT oil, except for acetaldehyde, which exhibited similar volatility in both oils. The same matrix effect was reported by Chaintreau et al. (*32*) with 2-butanone when comparing MCT ($K = 1.4 \times 10^{-3}$) and soja oils ($K = 2.6 \times 10^{-3}$) at 30 °C. The MCT oil used in the

present work included caprylic (C8) and capric (C10) fatty acids at 60 and 40%, respectively. The averaged sunflower oil composition was dominated by C18:1 and C18:2 fatty acids, at 20 and 67%, respectively (*33*). Consequently, sunflower oil, like soya oil, should exhibit a higher hydrophobicity than MCT oil. However, most of the volatiles should have a higher affinity for oils of higher hydrophobicity and consequently a lower volatility. Rabe et al. (*34*) came to the same conclusion with o/w emulsions and showed that the molarity of the lipid phase, i.e., the number of oil particles, played a dominant role on the release process of flavors under static and dynamic conditions. The differences in release from emulsions made with different oils (average carbon number: C9, C14, and C16) became nonsignificant for most of the compounds when the same molarity was applied for the different oils.

The measured air−oil partition coefficients measured in the present study were compared with the literature values. The highest temperatures found in the literature for the same compounds diluted in vegetable oils were 37 and 40 °C (*35*, *36*). The published data report lower partition coefficients than in the present work. This difference seemed linked to a temperature effect since increasing the temperature results in an increase in the air−liquid partition coefficients. Karl et al. (*24*) used the same device as described here and validated the dynamic stripping method interfaced with PTR-MS through a comparison of their volatility data obtained for alcohols, aldehydes, and ketones with data reported in the literature. The literature values were in good agreement with their experimental results obtained at the same temperature.

Aroma−Matrix Interactions. The procedure applied to isolate the aroma compounds by SPME was first optimized. A PDMS/CAR fiber was selected because it presents the highest capacity to adsorb and was the most sensitive to small molecules such as acetaldehyde and methyl formate. Equilibration times from 15 to 60 min provided reproducible peak areas by GC-MS. Thus, an equilibration time of 15 min was chosen for all of the samples at 70 °C. Finally, the linearity of detection of the volatile compounds desorbed from the PDMS/CAR fiber was satisfactory in our experimental conditions with linear correlation coefficients from 0.88 to 0.98.

The occurrence of interactions between the aroma compounds and a structured model system was determined relative to the release in the reference system, i.e., pure MCT or sunflower oil (**Table 2**). A release percentage significantly lower than 100% (reference) indicated a retention of the aroma compound by the structured oil system.

The lowest relative retentions were observed for acetaldehyde, methyl formate, butanol, and octanol. The volatile retention was generally more pronounced in the presence of sunflower oil. Acetaldehyde release was greatly reduced (35−49% release relative to both bulk oils) in both the L_2 phase and the w/o emulsion. The methyl formate release was characterized by a large decrease in the w/o emulsion (only 11% release in the w/o emulsion relatively to the release in sunflower oil), while butanol and octanol were better retained in the L_2 phase (33 and 35% release in the L_2 phase relatively to the release from sunflower oil). The release of the other volatiles was similar from the L_2 phase and the w/o emulsion or differed significantly. The release of ethyl acetate, hexanal, ethyl butanoate, nonanal, and decanal varied from 73 to 125%, which demonstrated a low retention or even no retention at all by the structured oil systems.

Four compounds, i.e., acetaldehyde, methyl formate, butanol, and octanol, behaved in structured oil systems differently from the other compounds. Acetaldehyde was well-retained most likely due to the hydrophilic domains present in both the emulsion and the microemulsion systems, while methyl formate was particularly retained by the hydrophilic domains of only the w/o emulsion. The release of butanol and octanol decreased strongly in the L_2 phase. This particular behavior was not observed for the other compounds having a similar hydrophobicity.

Table 2. Release (%)[a] of the Aroma Compounds in the L_2 Phases and w/o Emulsions Relative to MCT or Sunflower Bulk Oil, Obtained by SPME Headspace Analysis

		oil used in model systems	
compound	system ratio	MCT oil	sunflower oil
acetaldehyde	oil	100 a	100 a
	L_2 phase/oil	35 b	36 b
	w/o emulsion/oil	41 b	49 c
melthyl formate	oil	100 a	100 a
	L_2 phase/oil	74 b	64 b
	w/o emulsion/oil	48 c	11 c
butanol	oil	100 a	100 a
	L_2 phase/oil	42 b	33 b
	w/o emulsion/oil	84 c	84 c
ethyl acetate	oil	100 a	100 a
	L_2 phase/oil	100 a	93 b
	w/o emulsion/oil	93 b	98 a
hexanal	oil	100 a	100 a
	L_2 phase/oil	74 b	73 b
	w/o emulsion/oil	76 b	89 a
ethyl butanoate	oil	100 a	100 a
	L_2 phase/oil	125 b	109 b
	w/o emulsion/oil	95 c	101 a
octanol	oil	100 a	100 a
	L_2 phase/oil	55 b	35 b
	w/o emulsion/oil	94 a	100 a
nonanal	oil	100 ab	100 a
	L_2 phase/oil	96 a	92 b
	w/o emulsion/oil	102 b	114 c
decanal	oil	100 a	100 a
	L_2 phase/oil	91 b	90 b
	w/o emulsion/oil	96 ab	112 a

[a] Data for one compound with different letters in the same column are significantly different ($p < 0.05$).

The correlations between the retention data and the log *P* values were investigated in more detail. Correlation coefficients of 0.4 and 0.8 were found for the L_2 phase and the w/o emulsion, for all of the compounds studied and irrespective of oil nature, respectively. For the L_2 phase, a better correlation occurred when considering each homologous series separately ($r \geq 0.97$ for esters and aldehydes). The interactions between the aroma compounds and the constituents of the L_2 phase are very specific and depend on the chemical function and the carbon chain length of the compounds. The volatile retention in both structured emulsions increased as the compound hydrophobicity (or log *P* value) decreased, i.e., as the compound became more hydrophilic. On the one hand, the hydrophilic domains of the L_2 phase and w/o emulsion increased the retention of hydrophilic compounds. The hydrophilic domains consist of the water droplets, which are stabilized by an emulsifier interfacial layer. On the other hand, the hydrophobic continuous phase of these systems seemed to behave as a bulk oil phase for hydrophobic compounds. Only compounds that present a certain amphiphilic structure, such as butanol and hexanol, appeared to be retained more by the microemulsion than by the emulsion system. The higher interfacial area of the microemulsion could be the characteristic that explains this observation.

The interactions between the aroma compounds and the emulsifiers diluted in oil, in the absence of dispersed water

Table 3. Release (%)[a] of the Aroma Compounds in Mixtures of Oil and 60% Monoglycerides (Oil-MG) and Mixtures of Oil and 5% PGPR (Oil-PGPR), Relative to MCT or Sunflower Bulk Oil, Obtained by SPME Headspace Analysis

		oil used in model systems	
compound	system ratio	MCT oil	sunflower oil
acetaldehyde	oil	100 a	100 a
	oil-MG/oil	59 b	70 b
	oil-PGPR/oil	96 a	102 a
methyl formate	oil	100 a	100 a
	oil-MG/oil	103 a	96 ab
	oil-PGPR/oil	113 a	95 b
butanol	oil	100 a	100 a
	oil-MG/oil	57 b	45 b
	oil-PGPR/oil	103 c	98 a
ethyl acetate	oil	100 ab	100 a
	oil-MG/oil	101 b	96 b
	oil-PGPR/oil	104 a	100 a
hexanal	oil	100 a	100 a
	oil-MG/oil	78 b	84 b
	oil-PGPR/oil	106 a	115 c
ethyl butanoate	oil	100 a	100 a
	oil-MG/oil	116 b	110 b
	oil-PGPR/oil	108 a	110 b
octanol	oil	100 a	100 a
	oil-MG/oil	66 b	47 b
	oil-PGPR/oil	114 a	119 a
nonanal	oil	100 a	100 a
	oil-MG/oil	86 b	87 a
	oil-PGPR/oil	111 a	128 b
decanal	oil	100 a	100 a
	oil-MG/oil	82 b	82 a
	oil-PGPR/oil	113 a	126 b

[a] Data for one compound with different letters in the same column are significantly different ($p < 0.05$).

droplets, were examined in order to evaluate the role of the structured system composition on the aroma release (**Table 3**). The presence of 5% PGPR in oil induced only a low variation of the aroma compound release relatively to the reference system. No strong influence of PGPR on the aroma release was detected. Therefore, in the case of the PGPR-stabilized w/o emulsion, the dispersed water droplets were responsible for the increased retention of acetaldehyde, methyl formate, and butanol measured (**Table 2**). However, the addition of 60% monoglycerides in oil significantly reduced the release of acetaldehyde, butanol, and octanol. For these aroma compounds, the retention observed in the L_2 phase could be partially explained by interactions with the monoglycerides.

Identification of the Ions Monitored by PTR-MS. The compound concentration was adjusted to minimize the interferences between fragment or parent ions of the different molecules and hence ensure a good correlation of each monitored ion for the assigned molecule. For instance, the *m*/*z* 89 ion is the parent ion of ethyl acetate as well as a fragment ion of ethyl butanoate. The ethyl butanoate concentration was then decreased to 5 μL/L, i.e., 10-fold lower than the ethyl acetate concentration to limit the overlapping of the *m*/*z* 89 ion.

As a one-dimensional technique, PTR-MS characterizes the detected compounds only via the recorded masses. The combination of a volatile separation by GC with a simultaneous and parallel detection by PTR-MS and EI-MS enabled (i) the identification the molecules released (added molecules and their possible impurities) and (ii) the interpretation of the on-line spectra obtained by PTR-MS.

The monitored masses contributed between 72 and 100% of the assigned volatile compounds released from the different systems. The lowest contribution of a mass to a volatile compound corresponded to the ion signal at *m*/*z* 33 for the methyl formate molecule with a variation of 72−76% of the whole spectrum. The occurrence of methanol, i.e., a methyl formate impurity, explains this lower but reliable contribution. The GC-PTR-MS data were not reproducible for the *m*/*z* 33 ion when using the w/o emulsions made from MCT or sunflower oil (0−45% contribution); therefore, the data from w/o emulsions were not taken into account in **Table 3**.

This finding, obtained under dynamic conditions, is in agreement with the retention data (**Table 2**). The retention of methyl formate by the w/o emulsions was particularly high and led to 11 and 48% release from the emulsions made from MCT and sunflower oil, respectively. Methyl formate could be partially hydrolyzed in the water droplets and/or involved in specific interactions within these emulsions. In the case of *m*/*z* 33 ion, the dynamic release curves of the w/o emulsions were not considered since they corresponded to methanol rather than to methyl formate.

Parameters Extracted from the On-line Release Curves. The parameters first extracted from the release curves were the following: the linear release rate over initial 15, 30, and 60 s; the maximum aroma intensity (I_{max}); the time needed to reach I_{max} (t_{max}); the rate to reach I_{max} (I_{max}/t_{max}); and the area under the curve between 0 and 15 s, 0−30 s, 0−60 s, and 0−10 min. The discriminative character of the extracted parameters from the release curves was investigated. The discrimination power of each parameter was given by the *F* ratio calculated as a one-way analysis of variance (data not shown). The *F* value is expressed by the ratio of the parameter variation between the oily systems to the parameter variation within these systems. Therefore, the discrimination power of each parameter increases with the *F* ratio value. The t_{max} parameter, although showing the lowest *F* ratio due to high variability, expressed the time needed to reach I_{max} and could then reveal a possible delay in the release of the volatile compounds. The I_{max} parameter had the highest *F* ratio. The rate I_{max}/t_{max} was not selected because of low discrimination power due to the high variability of t_{max}.

The second criterion used to select consistent parameters was the occurrence of internal correlations between the different extracted parameters (data not shown). The linear rates over initial 30 and 60 s, as well as the areas between 0 and 30 and 0−60 s, were positively and highly correlated to I_{max}. On the contrary, the very initial release behavior (15 s) was not well-represented by I_{max}. The three areas between 0 and 15, 0 and 30, and 0 and 60 s were highly correlated to each other as well as to the rate over 15 s.

Conclusively, the selected extracted parameters were the linear release rate over 15 s (rate 15), I_{max}, t_{max}, and the area under the curve from 0 to 10 min (area 0−10), which represented the overall release intensity (**Tables 4** and **5**).

The rate 15, I_{max}, and area 0−10 parameters obtained in structured systems made from MCT oil were similar or significantly higher than the parameters obtained from the pure MCT oil (ratio ≥100) and particularly in the case of area 0−10 (ratios >300) (**Table 4**). The temporal release of the volatiles from the L_2 phase and the w/o emulsion was hence characterized by a fast initial release over the first 15 s and a higher concentration in the headspace (I_{max} and area 0−10).

The t_{max} ratios for the L_2 phase and the w/o emulsion were lower or equal to 100. Some aroma compounds, i.e., octanol, nonanal, and decanal, were therefore released faster from the studied structured systems than from the pure MCT oil (**Table 4**).

Table 4. Ratios[a] of the Parameters Extracted from the PTR-MS Kinetic Release Curves Obtained from the L_2 Phase (MCT-L_2), w/o Emulsion (MCT-w/o), and Pure Oil, with MCT as the Oil Phase

	MCT-L_2/MCT				MCT-w/o/MCT			
ion (*m/z*)	rate 15	I_{max}	t_{max}	area 0–10	rate 15	I_{max}	t_{max}	area 0–10
33	222 (109)	141 (41)	100 (47)	154 (26)				
45	174 (77)	112 (34)	116 (45)	408 (110)	245 (67)	142 (40)	107 (32)	454 (158)
57	149 (59)	92 (17)	101 (25)	367 (51)	242 (63)	153 (28)	78 (39)	572 (112)
71	127 (36)	96 (10)	60 (26)	376 (34)	203 (48)	144 (9)	26 (12)	560 (55)
89	271 (139)	162 (37)	120 (40)	625 (123)	308 (98)	173 (44)	133 (44)	610 (181)
101	283 (141)	157 (32)	110 (48)	631 (111)	300 (127)	161 (36)	75 (36)	608 (133)
117	373 (180)	182 (26)	79 (29)	746 (112)	339 (128)	174 (28)	133 (48)	655 (135)
143	243 (89)	157 (20)	38 (22)	664 (84)	225 (70)	146 (14)	39 (28)	592 (82)
157	174 (60)	145 (21)	57 (43)	639 (80)	178 (45)	134 (15)	37 (25)	560 (70)

[a] Data between parentheses correspond to the 95% confidence intervals of the ratio.

Table 5. Ratios[a] of the Parameters Extracted from the PTR-MS Kinetic Release Curves Obtained from the L_2 Phase (SF-L_2), w/o Emulsion (SF-w/o), and Pure Oil, with Sunflower Oil (SF) as the Oil Phase

	SF-L_2/SF				SF-w/o/SF			
ion (*m/z*)	rate	I_{max}	t_{max}	area 0–10	rate	I_{max}	t_{max}	area 0–10
33	200 (52)	102 (28)	57 (16)	110 (39)				
45	154 (45)	88 (28)	73 (23)	90 (35)	197 (71)	98 (18)	73 (30)	100 (28)
57	106 (41)	59 (5)	91 (44)	60 (10)	216 (73)	115 (9)	70 (21)	116 (18)
71	109 (38)	65 (8)	64 (37)	63 (9)	219 (69)	127 (14)	60 (36)	123 (18)
89	205 (78)	116 (11)	89 (43)	114 (23)	231 (91)	118 (12)	111 (34)	119 (33)
101	218 (99)	125 (17)	37 (14)	124 (24)	239 (102)	127 (13)	44 (20)	130 (27)
117	241 (119)	133 (17)	66 (26)	134 (23)	257 (94)	129 (18)	55 (19)	129 (26)
143	224 (98)	132 (12)	75 (39)	134 (21)	245 (92)	131 (15)	73 (37)	133 (22)
157	188 (65)	133 (16)	71 (41)	135 (20)	204 (70)	132 (18)	41 (20)	133 (20)

[a] Data between parentheses correspond to the 95% confidence intervals of the ratio.

The use of sunflower oil in the structured lipid systems generally led to smaller parameter ratios (**Table 5**). The differences of dynamic release behavior between the structured emulsions and the pure oil were reduced in the presence of sunflower oil. The release trends observed for MCT oil systems remained valid. The rate 15, I_{max}, and area 0−10 parameters were significantly higher or similar to those obtained from pure sunflower oil, whereas the t_{max} value was significantly lower or similar to that obtained from the pure oil. Overall, the parameter ratios seemed to demonstrate a greater influence of the oil nature on the release difference between structured and nonstructured systems than the system structure itself, i.e., whether the system contained microdroplets or nanodroplets of water. As an exception to this observation, the release of butanol and octanol was highly affected by the system structure in the presence of sunflower oil. Their I_{max} and area 0−10 ratios were much lower in the L_2 phase than in the w/o emulsion (**Table 5**). The specific dynamic release behavior of the two alcohols could be explained by an important retention of these compounds by the L_2 phase (**Table 2**).

The effect of the volatile compound properties on the dynamic release was then particularly examined by plotting the four parameter ratios as a function of the volatile compound hydrophobicity and their retention data.

Correlation between Dynamic Release Parameters and Physicochemical Characteristics of the Aroma Compounds. **Table 6** displays the correlation coefficients obtained between the parameters extracted from the release curves and interaction data (release percentage at equilibrium). The three parameters rate 15, I_{max}, and area 0−10 of the L_2 phases prepared with both oils were significantly and positively correlated to the interaction data of the aroma compounds (**Figure 1**). The differences in initial rate (rate 15) and headspace concentrations (I_{max} and area 0−10) between the L_2 phases and the oil increased when the aroma compound was less retained by the microemulsion, which was shown by the increasing ratios of the release percentages. The compound retention in the L_2 systems was a physicochemical characteristic, which could predict the initial release rate as well as the maximum intensity (I_{max}) and the total amount of compound released during 10 min. The log *P* values were poorly correlated to the ratios of rate 15, I_{max}, and area 0−10 corresponding to the L_2 phases ($-0.1 \leq r \leq 0.5$; data not shown). Under the dynamic conditions applied, the data accounting for interactions should be more effective to model the aroma release from L_2 phases.

Table 6. Correlation Coefficients[a] between the Flavor Release Parameters and the Interaction Data for the Four Model Systems: L_2 Phase and w/o Emulsion Made from MCT Oil (MCT-L_2 and MCT-w/o) and L_2 Phase and w/o Emulsion Made from Sunflower (SF) Oil (SF-L_2 and SF-w/o)

parameter	MCT-L_2/MCT	MCT-w/o/MCT	SF-L_2/SF	SF-w/o/SF
rate 15	0.80*	–0.07	0.90*	0.51
I_{max}	0.91*	0.17	0.93*	*0.90*
t_{max}	–0.32	–0.32	–0.08	–0.15
area 0–10	0.70*	*0.75*	0.91*	*0.91*

[a] Significant correlation ($n = 9$): *, $p < 0.05$. Data in italics were significantly different at $p < 0.05$, but the plot of the data sets did not result in a linear regression of the points.

Regarding the w/o emulsions, no significant or consistent correlation was found between the release curve parameters and the retention data. Interactions between aroma compounds and the L_2 phase seemed to be particularly strong and specific to induce an effect on the aroma release rate and intensity. Instead of interactions, other thermodynamic and/or kinetic components

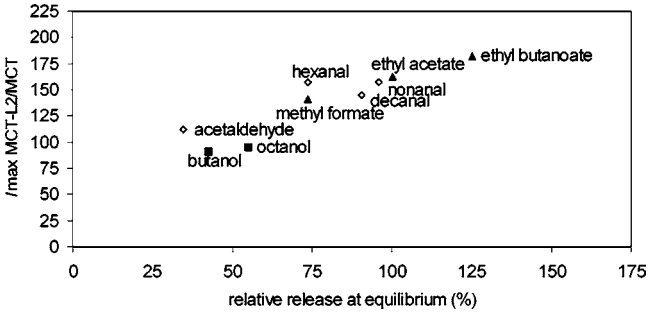

Figure 1. Ratio of I_{max} values obtained from the dynamic headspace analysis of the L_2 phase (MCT oil) and pure MCT oil, as a function of the relative release of the aroma compounds at equilibrium in the same systems.

of the flavor release could drive the release from the w/o emulsions. Rabe et al. (*37*) showed that the initial dynamic flavor release in o/w emulsions was dominated by the experimental oil/water partition coefficient of the volatiles, which was consequently used to replace the theoretical octanol/water partition coefficients and improve the modeling and prediction of the release. The volatile concentration in the continuous oil phase of the w/o emulsions determined by the liquid/liquid partition coefficient could then be of greater importance for the release than the relative amount of volatiles in headspace. The kinetic properties of the aroma compounds, i.e., their diffusion and mass transfer coefficients, into the w/o emulsions should also be considered in this dynamic process. Kinetic properties are affected by the medium texture and microstructure (*38*). However, the viscosity of the L_2 phase and w/o emulsion differed to a low extent at 70 °C. The emulsion microstructure is then more likely to be the kinetic factor that would explain the differences of correlation observed between the two emulsions.

A significant and negative correlation was established between t_{max} and log P for the L_2 phase ($r = -0.85$) and w/o emulsion ($r = -0.78$) made from MCT oil. The t_{max} values obtained for these structured multiphasic systems decreased relative to the pure MCT oil as the compound hydrophobicity increased. A faster release from the L_2 phase and w/o emulsion made from MCT oil was then observed for hydrophobic compounds, i.e., octanol, nonanal, and decanal. Conversely, the t_{max} parameter of the rather hydrophilic compounds (log $P \leq 2$) was not significantly different from the one determined in pure MCT oil (**Table 4**).

The more lipophilic molecules were faster released from the L_2 phase and the w/o emulsion, which could be the result of an exclusion volume effect. The presence of the respective nanometer and micrometer-sized water droplets reduces the continuous oily domain. Therefore, the initial concentration of the solubilized hydrophobic volatiles in the oily domain can be relatively higher than in pure oil. Salvador et al. (*39*) also proposed the occurrence of an exclusion volume effect to explain the faster release rate of diacetyl from o/w emulsion than from water. However, factors such as increased surface area and dynamics of the emulsion also have to be considered. A second hypothesis specific to the L_2 phase structure is linked to its particular structured lipophilic domain constituted by the spontaneous and stable interactions between the oil triglycerides and the free or adsorbed monoglycerides. Such a structure should reduce the volume of free lipid molecules and would inhibit the solubilization of hydrophobic solutes in the continuous lipid phase. As a consequence, in both structured systems, the maximum concentration of the more lipophilic compounds in the vapor phase would be reached faster.

No correlation between t_{max} and log P was demonstrated for systems made from sunflower oil ($r = -0.1$ for the L_2 phase; $r = -0.5$ for the w/o emulsion). In addition, most of the t_{max} ratios were less than 100 in the presence of sunflower oil ($p \leq 0.05$) (**Table 5**). The time to reach I_{max} was shorter for the structured systems made with sunflower oil than for the pure oil, whatever the compound hydrophobicity. The oil nature seemed to affect greatly the influence of the volatile physicochemical properties on t_{max}. The oil hydrophobicity, molarity, and composition (chain length, unsaturation degree, position of the esterified fatty acids) may be important factors involved in thermodynamic and kinetic processes of aroma release (*34*).

A third set of correlation was found for the w/o emulsion made from sunflower oil (i) between I_{max} and log P ($r = 0.83$) and (ii) between area 0−10 and log P ($r = 0.84$). The same correlations were reported for the L_2 phase made from sunflower oil when butanol and octanol were omitted ($r = 0.84$). When searching for correlations between the dynamic parameters and log P, an effect of the oil nature on the dynamic release of the volatiles was demonstrated, which seemed independent of the emulsion structure.

Overall, on the one hand, the correlation between the t_{max}, I_{max}, and area 0−10 parameters and the log P depended on the oil used. Moreover, the correlation between rate 15, I_{max}, and area 0−10 and the interaction data dealt with one type of structure, i.e., the microemulsion structure. This tendency could help to better select the oils or structures based, respectively, on the hydrophobicity or retention data of aroma compounds. This study was limited to two different oils and structured systems, which means that an instrumental and sensory validation should be performed on a larger range of oils and oil-based structured systems.

This work provides indications for potential applications of the w/o emulsion and the L_2 phase as aroma delivery systems when diluted in food products to improve retronasal or orthonasal perception. Upon dilution, the structured emulsions prepared from MCT oil would provide a faster release of aroma burst involving hydrophobic compounds and when prepared with sunflower oil a higher and sustained concentration in headspace of hydrophobic volatiles in the headspace (except alcohols in L_2 phase). Focusing on the L_2 phase, preliminary retention information is required in order to better predict the release patterns of volatiles of interest, i.e., initial release rate, aroma burst concentration, and overall released amount. Therefore, the selection of oils and structures should consider the targeted temporal release patterns of aroma in the headspace, e.g., whether a fast aroma burst is preferred rather than a delayed one and for which aroma compounds.

LITERATURE CITED

(1) Baek, I.; Linforth, R. S. T.; Blake, A.; Taylor, A. J. Sensory perception is related to the rate of change of volatile concentration in-nose during eating of model gels. *Chem. Senses* **1999**, *24*, 155−160.

(2) Kant, A.; Linforth, R. S. T.; Hort, J.; Taylor, A. J. Effect of β-cyclodextrin on aroma release and flavor perception. *J. Agric. Food Chem.* **2004**, *52*, 2028−2035.

(3) Taylor, A. J.; Alston, M. J.; Hemingway, K. M.; Chappel, C. G.; Mlotkiewicz, J. A. Flavour delivery systems comprising a microemulsion or hydrated reversed micelles. Patent application, WO 99/62357, 1999.

(4) Zeller, B.; Ceriali, S.; Wragg, A.; Gaonkar, A. G. Method of preparing coffee aromatizing compositions. Patent application, WO 02/058481, 2002.
(5) Doyen, K.; Carey, M.; Linforth, R. S. T.; Marin, M.; Taylor, A. J. Volatile release from an emulsion: Headspace and in-mouth studies. *J. Agric. Food Chem.* **2001**, *49*, 804−810.
(6) Roberts, D. D.; Pollien, P.; Antille, N.; Lindinger, C.; Yeretzian, C. Comparison of nosespace, headspace, and sensory intensity ratings for the evaluation of flavor adsorption by fat. *J. Agric. Food Chem.* **2003**, *51*, 3636−3642.
(7) van Ruth, S. M.; Buhr, K. Influence of saliva on temporal volatile flavour release from red bell peppers determined by proton transfer reaction-mass spectrometry. *Eur. Food Res. Technol.* **2003**, *216*, 220−223.
(8) Drewnowski, A. Sensory properties of fats and fat replacements. *Nutr. Rev.* **1992**, *50*, 17−20.
(9) Guyot, C.; Bonnafont, C.; Lesschaeve, I.; Issanchou, S.; Voilley, A.; Spinnler, H. E. Effect of fat content on odor intensity of three aroma compounds in model emulsions: δ-Decalactone, diacetyl, and butyric acid. *J. Agric. Food Chem.* **1996**, *44*, 2341−2348.
(10) Buttery, R. G.; Guadagni, D. G.; Ling, L. C. Flavor compounds volatilities in vegetable oil and oil-water mixtures: Estimation of odor thresholds. *J. Agric. Food Chem.* **1973**, *21*, 198−201.
(11) Landy, P.; Courthaudon, J. L.; Dubois, C.; Voilley, A. Effect of interface in model food emulsions on the volatility of aroma compounds. *J. Agric. Food Chem.* **1996**, *44*, 526−530.
(12) Bakker, J.; Mela, D. J. Effect of emulsion structure on flavor release and taste perception. In *Flavor-Food Interactions*; McGorrin, R. J., Leland, J. V., Eds.; ACS Symposium Series 633; American Chemical Society: Washington, DC, 1996; pp 36−47.
(13) Dickinson, E.; Evison, J.; Gramshaw, J. W.; Schowpe, D. Flavour release from a protein-stabilized water-in-oil-in-water emulsion. *Food Hydrocolloids* **1994**, *8*, 63−67.
(14) Haahr, A. M.; Bredie, W. L. P.; Stahnke, L. H.; Jensen, B.; Refsgaard, H. H. F. Flavour release of aldehydes and diacetyl in oil/water systems. *Food Chem.* **2000**, *71*, 355−362.
(15) Ubbink, J.; Schoonman, A. M. Flavor delivery systems. *Kirk-Othmer Encyclopedia of Chemical Technology*; Wiley: New York, 2003.
(16) Darling, D. F.; Izzard, M. J.; Povey, K. J. Hydratable powders which form w/o/w emulsions. U.S. Patent application, 4933192, 1990.
(17) Harvey, B.; Druaux, C.; Voilley, A. The effect of protein on the retention and transfer of aroma compounds at the lipid water interface. In *Food Macromolecules and Colloids*; Dickinson, E., Lorient, D., Eds.; The Royal Society of Chemistry: Cambridge, 1995; pp 154−163.
(18) Friberg, S. E.; Kayali, I. Surfactant association structures, microemulsions, and emulsions in foods. In *Microemulsions and Emulsions in Foods*; El-Nokaly, M., Cornell, D., Eds.; ACS Symposium Series 448; American Chemical Society: Washington, DC, 1990; pp 7−24.
(19) Leser, M. E.; Michel, M.; Watzke, H. J. Food goes nano−New horizons for food structure research. In *Food Colloids, Biopolymers and Materials*; Dickinson, E., Van Vliet, T., Eds.; The Royal Society of Chemistry: Cambridge, 2003; pp 3−13.
(20) Leser, M.; Vauthey, S. Food composition containing a monoglyceride mesomorphic phase. U.S. Patent application 6569478, 2003.
(21) Miller, M.; Akashe, A.; Das, D. Mesophase-stabilized emulsions and dispersions for use in low-fat and fat-free food products. U.S. Patent application 6068876, 2000.
(22) Leroi, J. C.; Masson, J. C.; Renon, H.; Fabries, J. F.; Sannier, H. Accurate measurement of activity coefficients at infinite dilution by inert gas stripping and gas chromatography. *Ind. Eng. Chem. Process. Des. Dev.* **1977**, *16*, 139−144.
(23) Mackay, D.; Shui, W.; Sutherland, R. Determination of air-water Henry's law constants for hydrophobic pollutants. *Environ. Sci. Technol.* **1979**, *13*, 333−337.
(24) Karl, T.; Yeretzian, C.; Jordan, A.; Lindinger, W. Dynamic measurements of partition coefficients using proton-transfer-reaction mass spectrometry (PTR-MS). *Int. J. Mass Spectrom.* **2003**, *223*−*224*, 383−395.
(25) Pollien, P.; Jordan, A.; Lindinger, W.; Yeretzian, C. Liquid-air partitioning of volatile compounds in coffee: Dynamic measurements using proton-transfer-reaction mass-spectrometry. *Int. J. Mass Spectrom.* **2003**, *228*, 69−80.
(26) Pollien, P.; Lindinger, C.; Yeretzian, C.; Blank, I. Proton transfer reaction mass spectrometry, a tool for on-line monitoring of acrylamide formation in the headspace of Maillard reaction systems and processed food. *Anal. Chem.* **2003**, *75*, 5488−5494.
(27) Lindinger, C.; Pollien, P.; Ali, S.; Yeretzian, C.; Blank, I.; Märk, T. Unambiguous identification of volatile organic compounds by proton-transfer reaction mass spectrometry coupled with GC/MS. *Anal. Chem.* **2005**, *77*, 4117−4124.
(28) Lindinger, C.; Pollien, P.; Ali, S.; Blank, I.; Märk, T. Direct inter-comparison of datasets obtained by different PTR-MS: A novel approach to optimize and adapt the fragmentation pattern using a standardization procedure. In *Proceedings of the 2nd International Conference on Proton Transfer Reaction Mass Spectrometry and Its Application*; Hansel, A., Märk, T., Eds.; Innsbruck University: Innsbruck, Austria, 2005; pp 89−95.
(29) Lindinger, W.; Hirber, J.; Paretzke, H. An ion/molecule-reaction mass spectrometer used for on-line trace gas analysis. *Int. J. Mass Spectrom. Ion Processes* **1993**, *129*, 79−88.
(30) Lindinger, W.; Hansel, A.; Jordan, A. On-line monitoring of volatile organic compounds at pptv levels by means of proton-transfer-reaction mass spectrometry (PTR-MS): Medical applications, food control and environmental research. *Int. J. Mass Spectrom. Ion Processes* **1998**, *173*, 191−241.
(31) Hintze, J. *Number Cruncher Statistical System*; Kaysville, Utah, 2001, www.NCSS.com.
(32) Chaintreau, A.; Grade, A.; Muňoz-Box, R. Determination of partition coefficients and quantitation of headspace volatile compounds. *Anal. Chem.* **1995**, *67*, 3300−3304.
(33) Rossell, B. *Oils and Fats Handbook*; Leatherhead Food RA: Leatherhead, United Kingdom, 1999.
(34) Rabe, S.; Krings, U.; Berger, R. G. Influence of oil-in-water emulsion characteristics on initial dynamic flavour release. *J. Sci. Food Agric.* **2003**, *83*, 1124−1133.
(35) Hall, G.; Andersson, J. Volatile fat oxidation products. II. Influence of temperature on volatility of saturated mono- and di-unsaturated aldehydes in liquid media. *Lebensm.-Wiss. Technol.* **1983**, *16*, 362−366.
(36) van Ruth, S. M.; Grossmann, I.; Geary, M.; Delahunty, C. M. Interactions between saliva and 20 aroma compounds in water and oil model systems. *J. Agric. Food Chem.* **2001**, *49*, 2409−2413.
(37) Rabe, S.; Krings, U.; Berger, R. G. Dynamic flavour release from Miglyol/water emulsions: Modelling and validation. *Food Chem.* **2004**, *84*, 117−125.
(38) de Roos, K. B. Effect of texture and microstructure on flavour retention and release. *Int. Dairy J.* **2003**, *13*, 593−605.
(39) Salvador, D.; Bakker, J.; Langley, K. R.; Potjewijd, R.; Martin, A.; Elmore, J. S. Flavour release of diacetyl from water, sunflower oil and emulsions in model systems. *Food Qual. Pref.* **1994**, *5*, 105−107.

Received for review September 15, 2006. Revised manuscript received December 7, 2006. Accepted December 27, 2006.

JF062643P